Mechanical Impact Performance of Additively Manufactured Negative Stiffness Honeycombs

Dixon Correa, Ken Bostwick, Preston S. Wilson, Michael Haberman, Carolyn Conner Seepersad
Mechanical Engineering Department and Applied Research Laboratories
The University of Texas at Austin

Abstract

Negative stiffness honeycombs materials are comprised of negative stiffness beams arranged in ordered arrays. They are capable of providing isolation from impacts and returning to their initial shape. Previous research by the authors focused on the behavior of negative stiffness honeycombs to quasi-static loading conditions. This paper investigates the behavior of similar negative stiffness honeycombs under impact. The construction of an impact testing rig for the experimental evaluation of negative stiffness honeycombs is discussed. Experimental results from impact tests performed on honeycomb prototypes manufactured using selective laser sintering (SLS) in nylon 11 material are presented and compared with analytical and finite element predictions as well as quasi-static test results.

Introduction

Protecting personnel or equipment from mechanical impact is highly important for a wide array of industries ranging from defense to commercial sporting goods. An ideal impact absorbing solution would dissipate large amounts of mechanical energy at a rate commensurate with the impact and then return to its original state in order to absorb any subsequent impacts. Traditional material solutions to address this need rely on either open- and closed-cell foams or more uniformly structured materials like honeycombs [1] [2]. Some foams, like those used in some athletic helmets, will return to their original shape after they are subjected to mechanical impacts because they are constructed from very soft polymer materials that can undergo large recoverable deformations via elastic buckling at the cell level. Unfortunately, the stiffness and specific energy absorbing capacity of soft polymer foams is very limited and thus not adequate to dissipate impacts in many applications [1]. Materials that demonstrate elevated capacity to absorb impacts, such as traditional honeycombs and metallic foams, derive their relevant properties from plastic buckling events at the cell level and display in-plane stress-strain response like that shown in Figure 1 where the energy absorbed is proportional to the area under the curve. The plastic deformation in the cell walls of those materials results in permanent deformation of the material after an impact, thereby sacrificing the ability to return to its original shape for an elevated capacity to absorb mechanical energy.

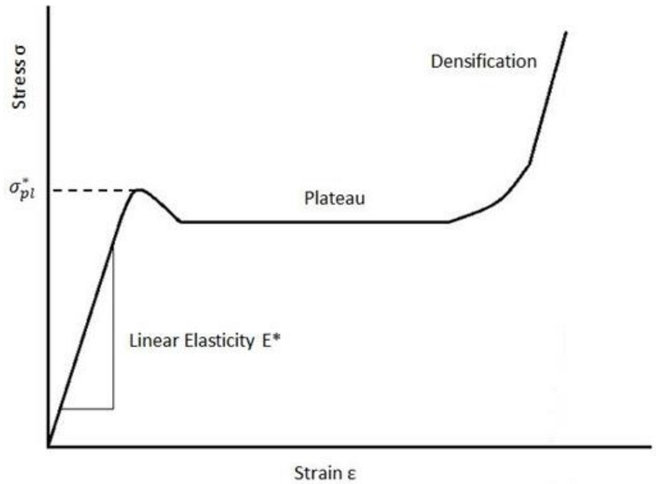

Figure 1. Stress-strain curve for a honeycomb in in-plane compression [2].

One potential material solution to address the shortcomings of soft material foams and plastically deforming foams or honeycombs is negative stiffness (NS) honeycombs [3] [4]. NS honeycombs are a new class of honeycomb material that utilize curved cell walls that are designed to generate high elastic stiffness under small levels of applied force and large deformation elastic buckling at elevated levels of applied force. An example NS honeycomb structure that was introduced and detailed by Correa et al [3] is shown in Figure 2. The horizontally-oriented walls of the NS honeycomb unit cell resemble two curved beams attached to each other via a vertical strut at their mid-point. When subjected to vertical displacement-controlled compressive loading, the cell walls first exhibit nearly linear elastic positive stiffness behavior associated with bending of the cell walls. Once the applied load reaches a threshold force, which is a function of the base material and cell geometry, the cell walls elastically buckle and the structure requires a *reduction* in the applied force to generate an *increased* displacement [5] [6], which is representative of negative stiffness behavior. Critically, if the unit cell geometry is designed appropriately, the NS honeycomb will return to its original configuration upon removal of the applied load and energy will be dissipated in the process. An experimentally obtained quasi-static force versus displacement curve that clearly illustrates this behavior is shown in Figure 4 for a nylon 11 NS honeycomb having the dimensions provided in Figure 3.

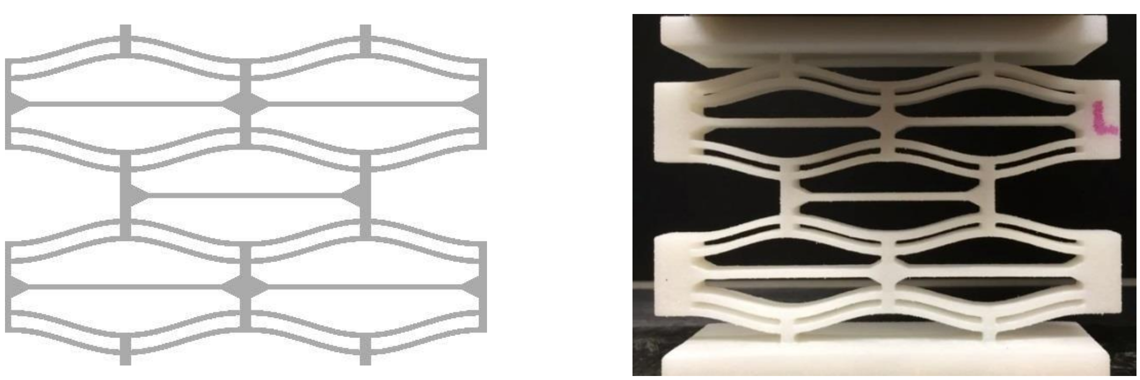

Figure 2. Schematic (L) and photograph (R) of a representative negative stiffness honeycomb. The honeycomb is fabricated with selective laser sintering in nylon 11 material [adapted from [3]].

The authors have previously explored the quasi-static large-deformation response of NS honeycombs using analytical, numerical, and experimental techniques [3] [4]. The results clearly demonstrated that NS honeycombs can be designed to yield specific energy absorbing capacity that is of the same order as traditional hexagonal honeycombs at low strain rates (10^{-4} s^{-1}) and that the NS honeycombs have the added benefit of returning to their original shape after the load is removed [4]. Further, previous related work showed that individual NS structures can be very effective mechanical isolators for both time-harmonic base vibration and impulsive motion [7]. The combination of those previous findings strongly suggests that NS honeycombs will be capable of providing impact isolation at elevated strain rate, although no experimental confirmation has yet been provided. While previous work suggests that effective absorption of impacts is possible using NS honeycombs, it is possible that high strain rate loading will diminish the performance of NS honeycombs. The current work therefore presents recent experimental findings on the response of NS honeycombs when subjected to uni-directional impact loading at strain rates up to 10^2 s^{-1}.

Experimental Methodology

The impact performance of the negative stiffness honeycombs was evaluated by subjecting additively manufactured honeycombs to controlled impacts using a specially constructed drop testing apparatus.

The negative stiffness honeycomb was additively manufactured with selective laser sintering on a 3D Systems Vanguard HiS+HiQ machine. The material was nylon 11 sourced from Applied Laser Materials as Arkema PA D80-ST unfilled nylon powder. By building several tensile bars near the honeycomb in the SLS build chamber, tension testing them, and averaging the results, the Young's modulus of the sintered nylon 11 material in the cell walls was estimated at 1582 MPa. Previously conducted quasi-static compression tests indicated a force threshold of approximately 200 N, at which point the negative stiffness unit cells begin to buckle elastically, as shown in Figure 4. The four top-most peaks in Figure 4 represent the sequential buckling of each row of curved beams in the honeycomb in Figure 2. The four bottom-most peaks represent the return of each row to its original position. The area bounded by the curves represents the energy absorbed by the honeycomb.

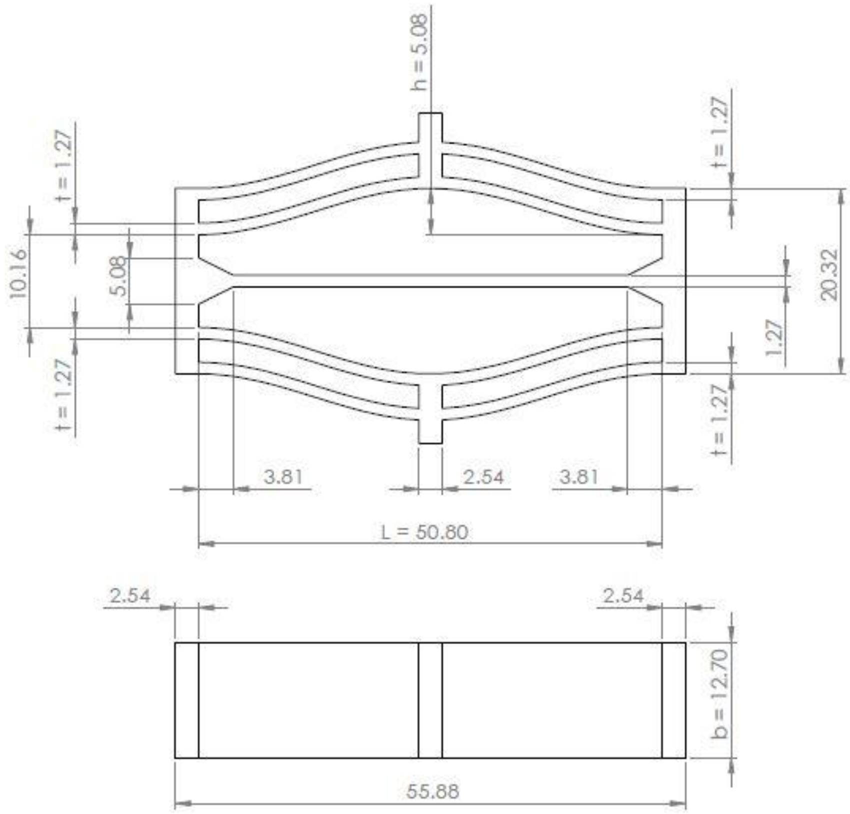

Figure 3. Geometry of a negative stiffness unit cell with dimensions in mm.

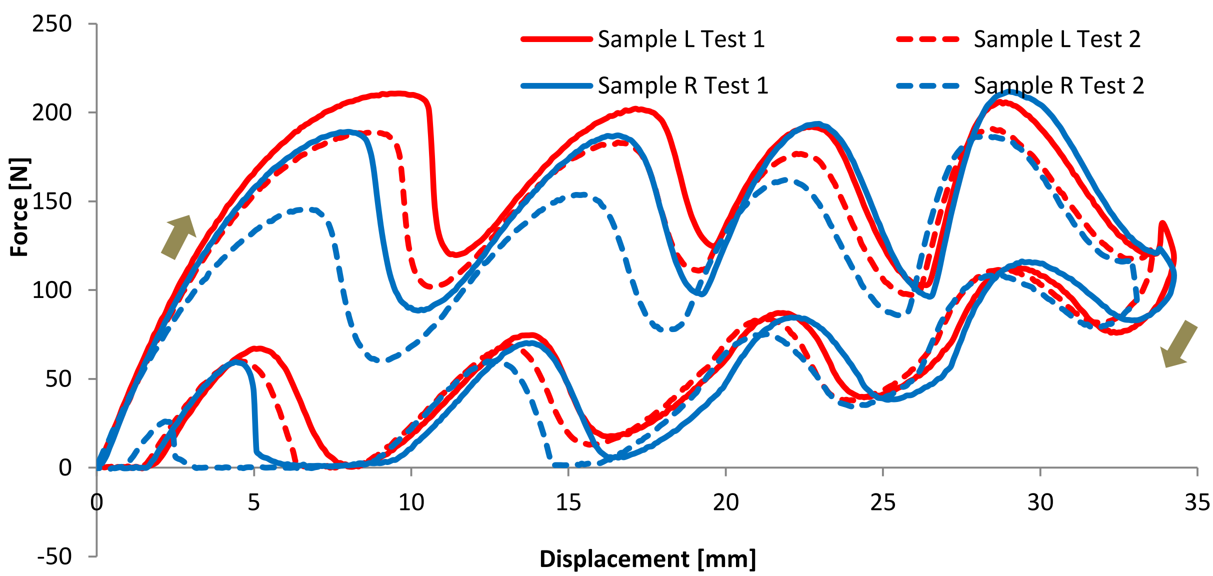

Figure 4. Force-displacement data from quasi-static compression tests of two negative stiffness honeycombs, indicating a force threshold of approximately 200 N.

Whereas the quasi-static compression tests were conducted at very low strain rates of approximately 10^{-4} s^{-1}, understanding the response of these honeycombs when subjected to impact required much higher strain rates of approximately 10^{2} s^{-1}. To conduct these tests, a custom impact testing apparatus was designed and constructed. A diagram of the impact testing apparatus is provided in Figure 5. The frame is constructed with one-inch-wide 80/20 extruded aluminum with supporting fasteners. The frame base (1) is rectangular with supporting feet that extend approximately 10 cm from the base for stabilization. Honeycomb specimens are fixtured to the base for impact testing. The honeycomb is impacted by an impact block (5) which travels along vertical guide rails (2) using lubricated ball rollers. Different impact blocks with different masses can be dropped from different heights to impart a wide variety of impact forces and velocities to the honeycombs. An accelerometer (PCB 352C03) is rigidly attached to the impact plate and collects data on the time history of acceleration of the plate. This data passes through a signal conditioner (PCB 482C) and data acquisition system (National Instruments NI 9234 DAQ card and cDAQ 9178 data acquisition system), and then it is recorded with a National Instruments LabView script.

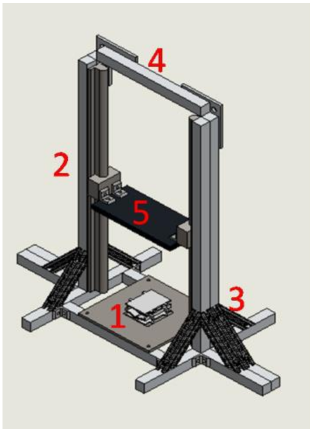

Figure 5. Impact testing apparatus.

Experimental Results

Impact testing was conducted by dropping an impact block with a mass of 1.8 kg from a variety of heights ranging from 11 to 40 cm and recording its acceleration history. Figures 6 and 7 document the time history of the 1.8 kg impact block falling from an initial height of 31 cm, with (Figure 6) and without (Figure 7) the honeycomb attached to the base plate. Acceleration data has been converted to force data in the figures by multiplying the acceleration data by the mass of the block. Figure 7 represents the entire time history of the block's impact with the unprotected base plate until it comes to rest, including several small bounces. Figure 6 represents the time history of the block's initial impact with the honeycomb; i.e., the first cycle of honeycomb compression and release. The astute reader will notice negative forces at the end of the time history plot in Figure 6; those negative forces are caused by gravity as the impact block bounces off the honeycomb after the first cycle of honeycomb compression and release and falls back toward the honeycomb for subsequent strikes before it eventually comes to rest. Secondary bounces are not represented in Figure 6.

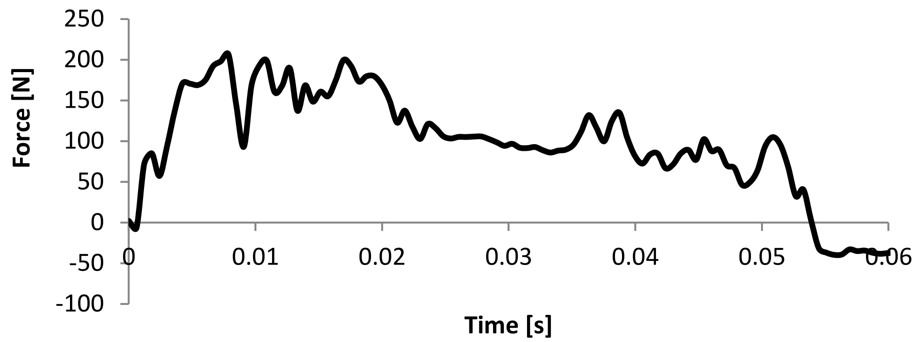

Figure 6. Time history of forces on the falling impact block with the honeycomb in Figure 2 fixtured to the base plate.

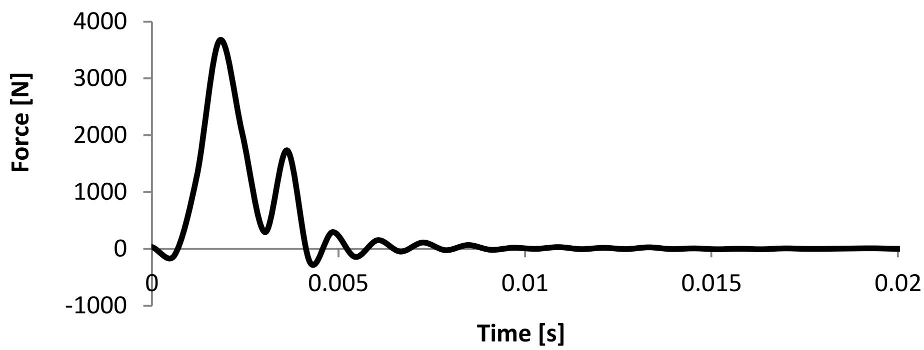

Figure 7. Time history of forces on the falling impact block with *no* honeycomb fixtured to the base plate.

A quick comparison of Figures 6 and 7 reveals that the presence of the honeycomb reduces the peak impact force from approximately 3600 N to approximately 200 N, a reduction factor of approximately 18. This reduction in peak impact force is accompanied by a temporal extension of the impact event. Without the honeycomb, the block comes to rest after 0.02 s, with most of the motion having subsided by 0.01 s. With the honeycomb in place, the block compresses and releases the honeycomb over a time period of approximately 0.05 s. Thereafter, the block bounces off the sample and strikes it repeatedly until it comes to rest. Only the first impact is illustrated in Figure 6. These results indicate that the honeycomb extends the duration of the impact, which, when combined with elastic deformation of the cell walls and the inherent loss factor of nylon 11, allows it to absorb energy at a much lower force threshold than that of a bare base plate.

It is also informative to interpret Figure 6 in terms of the physical movement of the honeycomb. In this case, the 31 cm drop of the 1.8 kg impact block provides enough energy to buckle three of the four rows of curved beams in the honeycomb. The three peaks with force thresholds of approximately 200 N in the first 0.02 s of impact are the peaks caused by the buckling of the first three rows of curved beams. The peaks between 0.035 and 0.05 s represent the beams snapping back to their original state. The reduced force thresholds in the snap back region are caused by hysteresis in the beams themselves. Specifically, since the beams are fabricated in a curved state, the force required to snap them through to their second stable buckled position is much higher than the force required to snap them back.

Figure 8 provides a comparison of the time history of the 1.8 kg block impacting the same honeycomb specimen from different heights. As the drop height is reduced, the energy from the impact buckles fewer rows of curved beams: 3 rows, 2 rows, and 1 row for the 31 cm, 21 cm, and 11 cm drop heights, respectively. It is also clear that the duration of the impact event decreases with decreasing impact height, as a result of buckling fewer rows of curved beams. Finally, regardless of the drop height, the force threshold is relatively constant at approximately 180-200 N. Figure 9 compares the time history of acceleration for the block impacting the unprotected base plate (in red) versus the time history of acceleration of the block impacting the honeycomb (in blue) for three different drop heights and illustrates the consistency and repeatability of the force threshold. The dotted green line represents an acceleration threshold of approximately 11 g's, which corresponds to the 200 N force threshold observed in previous plots. This consistency of force and acceleration thresholds indicates that the honeycombs are consistently clipping the magnitude of the force or acceleration transmitted through the honeycomb, regardless of the magnitude of the input energy. It also indicates that the performance of the honeycombs is repeatable and predictable, such that repeated tests give similar performance. Figure 10 reinforces the notion that the honeycomb behavior is repeatable. It represents repeated drop tests from a 30 cm drop height with (blue) and without (red) the honeycomb. The data indicates consistent time histories of acceleration and peak accelerations across multiple repetitions of the 30 cm impact.

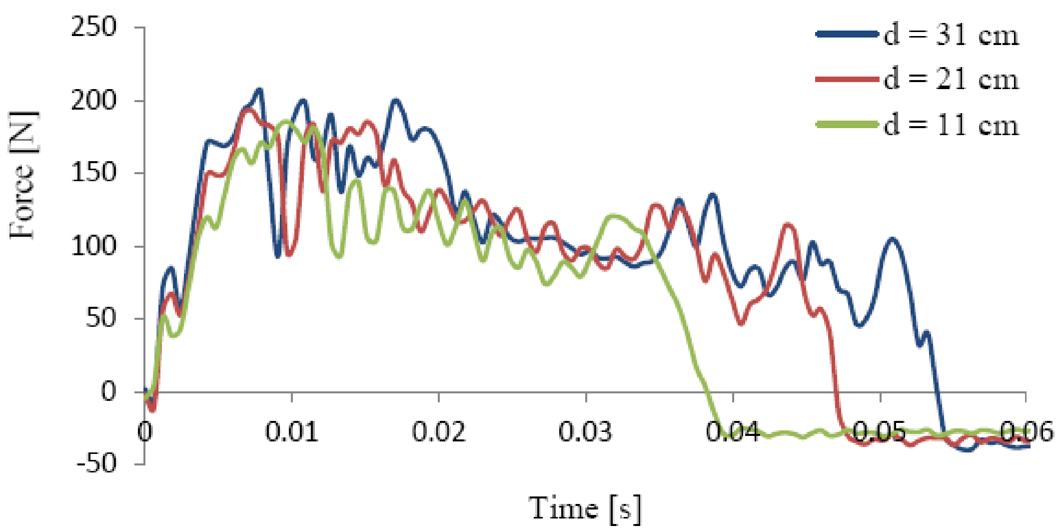

Figure 8. Time history of forces on the impact block as it impacts the honeycomb. The differently colored lines represent different drop heights.

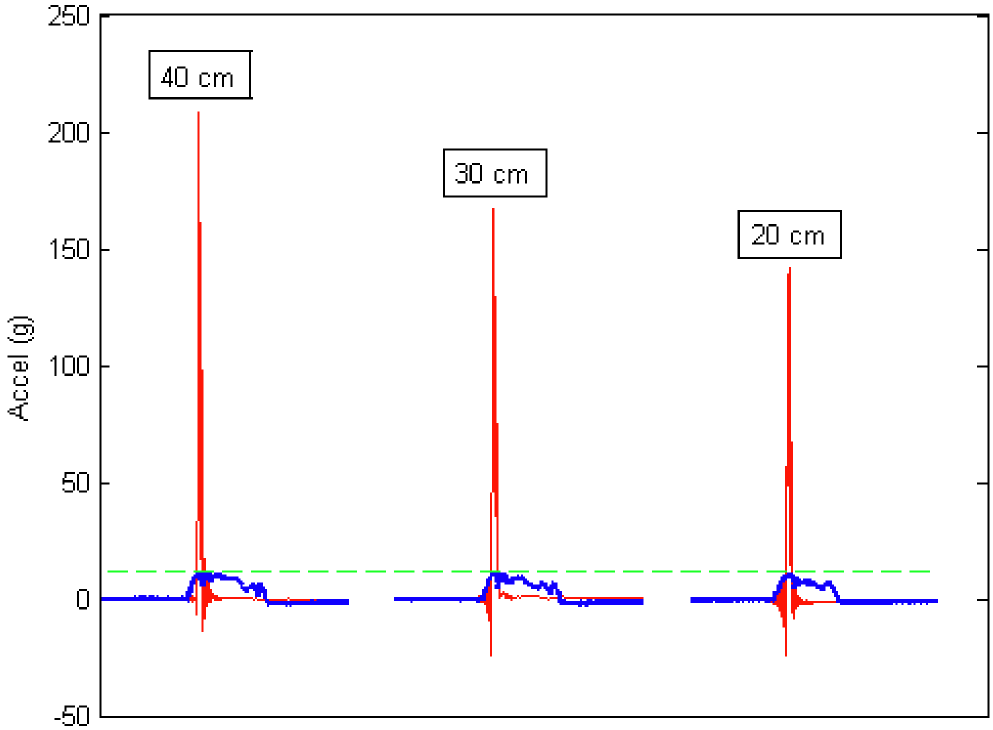

Figure 9. Plots of acceleration versus time for various drop heights. Red curves represent the acceleration of the 1.8 kg block impacting the unprotected base plate. Blue curves represent the block impacting the honeycomb detailed in Figures 2 and 3.

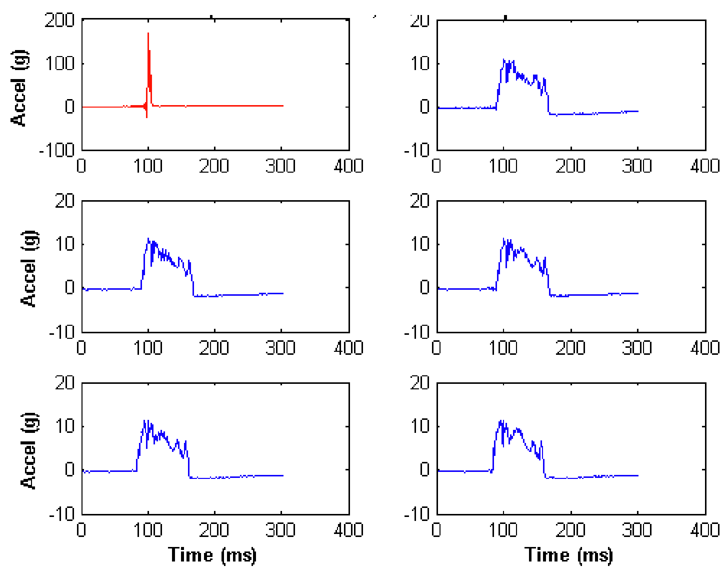

Figure 10. Plots of acceleration versus time for 30 cm drop heights with (blue) and without (red) the honeycomb on the base plate.

Comparison of Experimental Results with Finite Element Analysis

FE Setup for Dynamic Impact Loading

Finite element (FE) analysis of the negative stiffness honeycomb was performed in Abaqus CAE. As shown in Figure 11, a fixed constraint was provided to the flat bottom surface of the honeycomb imitating its resting position on the plate of the impact testing rig. The fixed constraint also helps mimic the clips that hold the honeycomb secure on the plate when impacted by the heavy block. Roller supports were provided to the outer cell walls and the cell junctions to model the effect of the central beam in the honeycomb cell. Further, it was determined that providing roller supports on either side of the beam connectors resulted in improved agreement between model and experimental results by virtue of forcing the beam to undergo third mode buckling. The falling block was modeled using a solid block with a fictitious density designed to match the mass of the block (1.8 kg) used in the experiment. This block was placed in assembly on the top flat surface of the honeycomb and given a velocity determined by the equation

$$v = \sqrt{2gd} \tag{1}$$

where v is the velocity of the block, g is the acceleration due to gravity, and d is the height above the honeycomb from which the block is dropped. The model assumes that there is negligible friction in the sliding bearings. For a setup that possesses significant frictional losses, the velocity may be predicted experimentally as described in the following section. A contact was created between the bottom surface of the falling block and the top flat surface of the honeycomb. Effects of strain hardening and viscoelasticity in the honeycomb were assumed to be negligible and were not included in the FE model. The honeycomb was meshed using a bottom-up mesh of hexahedral elements and the element size was set to 0.80 mm. The solver used for the dynamic simulation was Abaqus\Explicit. The force-time relationship for impact was derived by summing the forces in the nodes at the top surface of the honeycomb.

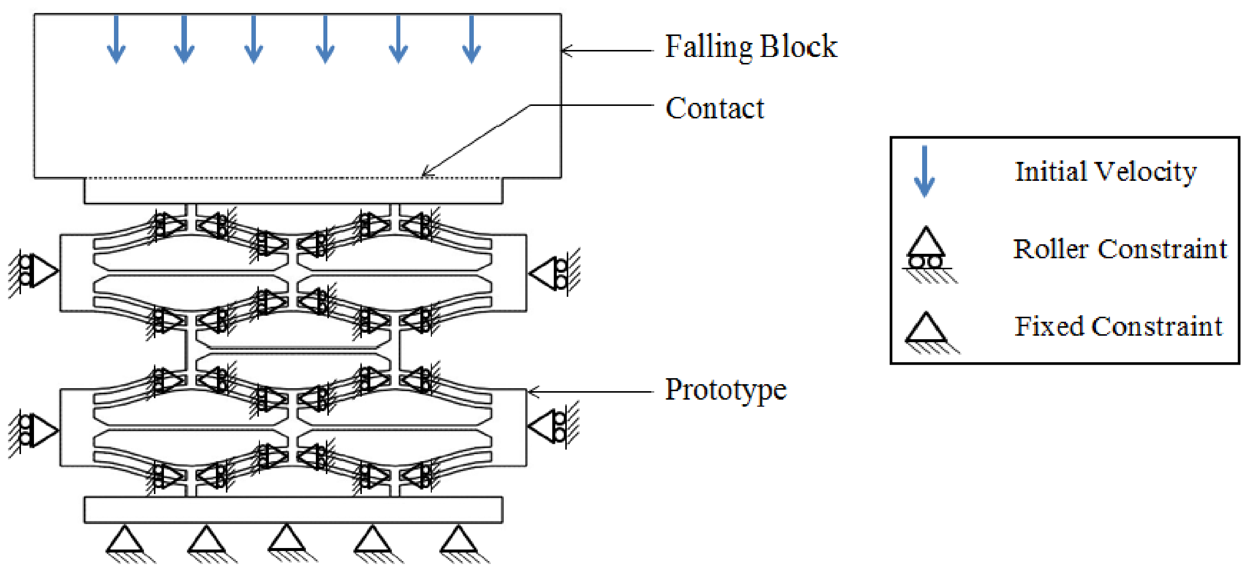

Figure 11. FE setup for dynamic impact loading of a negative stiffness honeycomb.

Comparison of FE and Experimental Results

Simulation results revealed that estimating block velocity using the equation given in Equation (1) was an over-estimation of the true velocity at impact because frictional bearing losses in the impact setup were significant. The true velocity of the block on impact with the honeycomb was measured experimentally using high speed photography as shown in Figure 12. The velocity measured was the average velocity of the block for its last 10 mm of travel. The camera was able to record the block traversing this distance in 7 frames. Based on the camera frame rate of 1200 fps, the velocity at impact was measured to be 1.71 m/s. This velocity was then used as an input in the FE simulation to predict the behavior of the honeycomb.

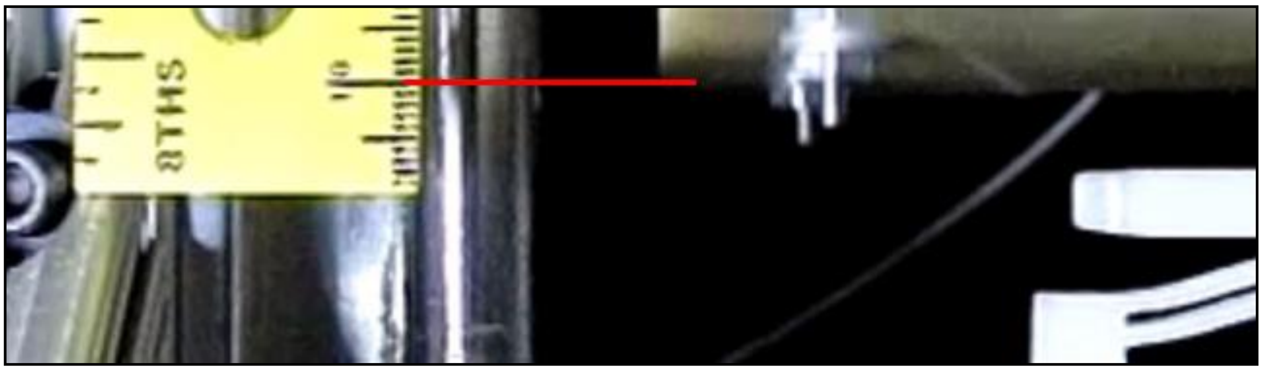

(a)

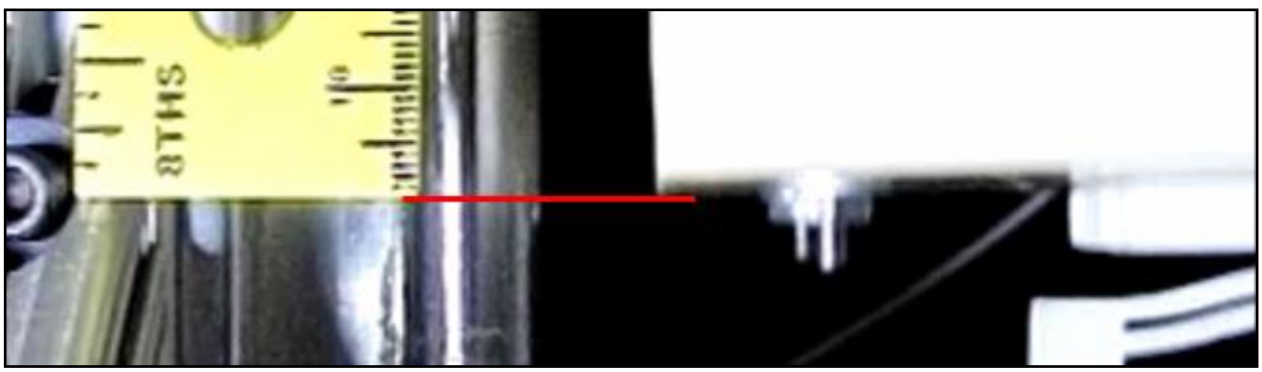

(b)

Figure 12. Experimental measurement of block velocity using high speed photography. (a) Block position 10 mm above honeycomb and (b) block position after 7 frames making initial contact with the honeycomb.

The FE prediction of the force-time relationship for the honeycomb under impact from a block with a velocity of 1.71 m/s is shown in Figure 13. The force data obtained from Abaqus was filtered using a second order low pass Butterworth filter, implemented in MATLAB with a cutoff frequency of 125 Hz. FE predicts that three rows of the honeycomb completely buckle when the block is dropped from this height, as indicated by the presence of three distinct peaks in the force-time relationship. Each peak represents a layer of the honeycomb buckling under impact from the falling block. The results predict a force threshold of approximately 200 N for each layer of the honeycomb, which is remarkably similar to the experimental results. However, the FE results exhibit peaks and valleys that are more prominent than the ones seen in the experimental results. This deviation may be due to the fact that effects of material damping were not implemented into the FE model but should be considered in future work. Another important similarity between the experimental and FE results is that the event durations for the buckling of the three rows of the honeycomb are similar. FE predicts an event duration of 0.025 seconds for the three layers to buckle which is approximately the same duration observed in experiments. The event durations for the bounce back observed in the latter half of the plot in Figure 13 are also similar. Overall, the accuracy of the FE results at this time are sufficient to predict the force threshold of a NS honeycomb design and provide estimates of its energy absorption capacity if the true block velocity is known. Future improvements to the FE model could include adding the effects of viscoelasticity in the base material of the NS honeycomb.

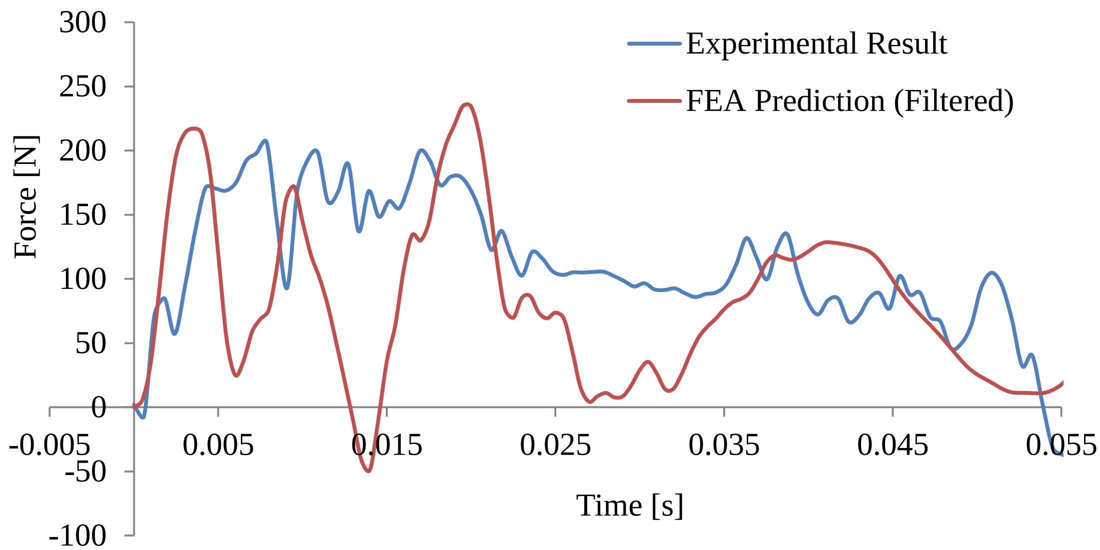

Figure 13. Experimentally obtained force-time relationship for a block dropped from a height of 31 cm above the honeycomb (d = 31 cm) versus filtered FE prediction considering block velocity v = 1.71 m/s.

Closure

This work presented experimentally obtained impact behavior of NS honeycombs fabricated from nylon 11 using selective laser sintering by employing a simple drop-test apparatus. The dynamic loading results, which imposed strain rates up to $10^2 s^{-1}$, have strong correlation with both finite element predictions and previously reported quasi-static loading tests which were performed at strain rates of approximately $10^{-4} s^{-1}$. The level of agreement between experiment and FE results is sufficient for the design of these types of materials for applications when recoverable impact isolation capabilities are of interest. Although the current FE predictions are adequate for design purposes, future FE modeling efforts should refine existing models to consider material relaxation effects for improved agreement between model and measurement and to provide a deeper understanding of these material structures. The strong agreement between the force thresholds observed in both quasi-static and impact loading scenarios suggests that rate dependence is not a major factor in NS honeycombs up to strain rates of $10^2 s^{-1}$, even when the base material is a viscoelastic material like nylon 11. To better understand rate dependence of NS honeycombs, future experimental work should focus on higher strain rate scenarios such as those experienced by a structure when exposed to blasts and measurements on NS honeycombs constructed from different base materials.

Overall, the experimental observations presented here indicate that NS honeycombs have a unique ability to provide rate-independent impact isolation capability and to subsequently recover from the associated deformation. This work therefore reinforces previous indications that NS honeycomb materials are compelling alternatives to traditional honeycombs because of their ability to absorb similar amounts of impact energy with NS honeycombs possessing the additional benefit of passively returning to their original shape.

Acknowledgements

The authors are grateful for support from DoD SBIR Program, Topic N142-085, in collaboration with Maritime Applied Physics Corporation. Tim Klatt was instrumental in developing initial honeycomb designs. Sergio Cortes and Professor Desiderio Kovar were very helpful in conducting quasi-static tests of the honeycombs.

References

[1] L. Gibson and M. Ashby, Cellular Solids: Structure and Properties, Cambridge, UK: Cambridge University Press, 1999.

[2] A. Hayes, A. Wang, B. Dempsey and D. McDowell, "Mechanics of Linear Cellular Alloys," *Mechanics of Materials,* vol. 36, pp. 691-713, 2004.

[3] D. Correa, T. Klatt, S. Cortes, M. Haberman, D. Kovar and C. Seepersad, "Negative Stiffness Honeycombs for Recoverable Shock Isolation," *Rapid Prototyping Journal,* vol. 21, no. 2, pp. 193-200, 2015.

[4] D. Correa, C. Seepersad and M. Haberman, "Mechanical Design of Negative Stiffness Honeycomb Materials," *Integrating Materials and Manufacturing Innovation,* vol. 4, no. 1, pp. 1-8, 2015.

[5] T. Klatt, M. Haberman and C. Seepersad, "Selective Laser Sintering of Negative Stiffness Mesostructures for Recoverable, Nearly-Ideal Shock Isolation," in *Proceedings of the Solid Freeform Fabrication Symposium*, Austin, TX, 2013.

[6] J. Qiu, J. Lang and A. Slocum, "A Curved-Beam Bistable Mechanism," *Journal of Microelectromechanical Systems,* vol. 13, no. 2, pp. 137-146, 2004.

[7] B. Fulcher, D. Shahan, M. Haberman, C. Seepersad and P. Wilson, "Analytical and Experimental Investigation of Buckled Beams as Negative Stiffness Elements for Passive Vibration and Shock Isolation," *Journal of Vibration and Acoustics,* vol. 136, no. 3, pp. 1-12, 2014.